atmosphere

MDPI

Article

A Novel Framework for Forecasting, Evaluation and Early-Warning for the Influence of PM_{10} on Public Health

Wendong Yang [1,2], Guolin Tang [1,2], Yan Hao [3] and Jianzhou Wang [4,*]

1 School of Management Science and Engineering, Shandong University of Finance and Economics, Jinan 250014, China; hshwendong@hotmail.com (W.Y.); guolin_tang@163.com (G.T.)
2 Institute of Marine Economy and Management, Shandong University of Finance and Economics, Jinan 250014, China
3 Business School, Shandong Normal University, Jinan 250014, China; yanhao0507@hotmail.com
4 Macau Institute of Systems Engineering, Macau University of Science and Technology, Macau 999078, China
* Correspondence: wjzdufe@gmail.com

Abstract: $PM_{2.5}$ has attracted widespread attention since the public has become aware of it, while attention to PM_{10} has started to wane. Considering the significance of PM_{10}, this study takes PM_{10} as the research object and raises a significant question: when will the influence of PM_{10} on public health end? To answer the abovementioned question, two promising research areas, i.e., air pollution forecasting and health effects analysis, are employed, and a novel hybrid framework is developed in this study, which consists of one effective model and one evaluation model. More specifically, this study first introduces one advanced optimization algorithm and cycle prediction theory into the grey forecasting model to develop an effective model for multistep forecasting of PM_{10}, which can achieve reasonable forecasting of PM_{10}. Then, an evaluation model is designed to evaluate the health effects and economic losses caused by PM_{10}. Considering the significance of providing the future impact of PM_{10} on public health, we extend our forecasting results to evaluate future changes in health effects and economic losses based on our proposed health economic losses evaluation model. Accordingly, policymakers can adjust current air pollution prevention plans and formulate new plans according to the results of forecasting, evaluation and early-warning. Empirical research shows that the developed framework is applicable in China and may become a promising technique to enrich the current research and meet the requirements of air quality management and haze governance.

Keywords: hybrid framework; forecasting; evaluation and early-warning; grey model; artificial intelligence optimization; health economic losses

Citation: Yang, W.; Tang, G.; Hao, Y.; Wang, J. A Novel Framework for Forecasting, Evaluation and Early-Warning for the Influence of PM_{10} on Public Health. *Atmosphere* **2021**, *12*, 1020. https://doi.org/10.3390/atmos12081020

Academic Editor: Rajasekhar Balasubramanian

Received: 2 August 2021
Accepted: 5 August 2021
Published: 9 August 2021

1. Introduction

The development of China's economy has brought about serious environmental problems, especially smog pollution, which is common in many cities in China, has a pernicious influence on public health and causes great economic losses and confusion in society. With the joint efforts of government, enterprises and the community, air quality can become much better and the influence of air pollution on public health can become increasingly smaller. However, one particular question remains to be answered: When will the influence of air pollution on public health end? $PM_{2.5}$ has attracted wide attention since it became known, while the attention paid to PM_{10} has started to wane.

PM_{10}, which is considered as one of the most dangerous air pollutants, is defined as particulate matter with an effective aerodynamic diameter of less than 10 μm [1]. As we all know, particulate matter can infiltrate the respiratory system and cause respiratory diseases [2]. In addition, there is a correlation between PM_{10} concentration levels and the number of hospitalizations for lung disease and heart disease [3]. However, due to natural resources, human activities, and chemical composition, some urban and rural areas report PM_{10} concentrations above the standard level. Specially, what is more serious is that existing research shows that even if the concentration of PM_{10} in the air is small, it will harm human health [4]. Therefore, in this context, to fill this research gap, this study takes PM_{10} as the research object and attempts to answer the question—"When will the influence of PM_{10} on public health end?"—using air pollution forecasting and health effects analysis, which present an extremely challenging task and can be considered a valuable area for further research.

To address air pollution forecasting issues, several models have been proposed to forecast the main pollutant concentrations and air quality index. For example, Xu et al. [5] proposed a hybrid system for forecasting daily concentrations of six air pollutants in three cities in China. Li and Jin [6] developed a novel forecasting model, which was applied in hourly pollutant concentration forecasting in Beijing, Tianjin, and Shijiazhuang, China. Similarly, Zhu et al. [7] presented a two-step hybrid model for forecasting daily average data of SO_2 and NO_2 in four cities in the region of central China. Liu et al. [8] devised an improved forecasting algorithm for air pollution forecasting based on the ensemble method. Hao and Tian [9] developed a multistep air quality forecasting model, which was applied to seven air quality signals and validated for cities in China. Xu [10] developed a model based on multiple kernel learning and weather data for forecasting air pollution $PM_{2.5}$ in Beijing. All the attempts indicate that hybrid models have become mainstream in forecasting air pollution and can be considered a promising tool to solve air pollution forecasting issues.

Furthermore, the review of the abovementioned studies shows that most of the previous studies are focused on air pollutant concentrations and air quality indices centered on hourly and daily data, which can provide the public with early warning information to protect them from the hazards of air pollution. However, the air quality management department cannot adjust their policies according to the forecasting results of a few hours or days in the future. Based on this, further studies focused on yearly data are a promising research direction to provide more valuable information and references for the related management department.

Although artificial intelligence models that exhibit better performance are widely used in many fields, such as mid-short-term load forecasting [11] and agricultural commodity futures prices prediction [12], they are not applicable to this study due to the limited data. In general, many other forecasting models are also not applicable. To develop an effective forecasting model, this study introduces the grey prediction theory into the forecasting model. Specifically, the first-order one-variable grey model, called GM (1, 1), is an effective forecasting model that can address forecasting issues with limited data and has been widely employed in many forecasting fields [13]. It has three benefits, namely it is very practical, has convenient operation, and high forecasting accuracy [14]. As a result, the GM (1, 1) model was selected as the basic forecasting engine to solve the forecasting issues with limited data in this paper. However, in addition, the individual grey model not only ignores the significance of optimization but also only performs better in the first step and performs worse as the forecasting horizon increases. Considering the promising potential of hybrid forecasting models and to remedy these limitations, this study introduces one advanced optimization algorithm and cycle prediction theory into the traditional GM (1, 1) model to develop an effective model for multistep forecasting of PM_{10} that can successfully obtain future changes in PM_{10}, provide guidance for the public to avoid health damage and economic loss, and help policymakers establish efficient policies and determine the proper method to control air pollution.

Another significant issue is the influence of PM_{10} on public health. How much losses have it caused in the past and future? To answer this question, the health economic losses assessment model was designed to evaluate the health effects and economic losses of pollution from PM_{10}. Specifically, air pollution's health effects and economic losses can be evaluated from the following three aspects: losses from premature death due to illness, medical expenses due to illness, and losses due to lost work. The developed evaluation model not only helps the public understand the basic conditions of health effects and economic losses, but also provides the conditions for the public to avoid damaging health and causing economic losses in the future. Most importantly, politicians can adjust their policies for the future according to the results of the evaluation.

In summary, in this paper, by combining the newly proposed forecasting model and evaluation model, a novel hybrid framework is developed for forecasting, evaluation, and early-warning for the influence of PM_{10} on public health. To verify the effectiveness of the developed hybrid framework of addressing air pollution issues and answering the research question, the PM_{10} concentration data in Xi'an, China is employed in this case study. Empirical research shows that the developed framework is applicable in China and may become a promising technique to enrich the current research and meet the requirements of air quality management and haze governance.

The remainder of this study is organized as follows. Section 2 develops the proposed hybrid framework for forecasting, evaluation, and early-warning. Section 3 conducts an empirical study. Discussion of the influence of the threshold value of PM_{10} is presented in Section 4. Finally, Section 5 concludes this paper.

2. The Developed Hybrid Framework for Forecasting, Evaluation, and Early-Warning

In this section, the hybrid framework for forecasting, evaluation and early-warning for the influence of PM_{10} on public health is developed, which consists of two parts: a novel forecasting model for PM_{10} and a novel assessment model for health economic loss.

2.1. Part I: A Novel Forecasting Model for PM_{10}

2.1.1. Grey Prediction Theory

Given a nonnegative time series $X^{(0)} = \left\{x^{(0)}(1),\, x^{(0)}(2),\, \ldots,\, x^{(0)}(n)\right\}$, where $n \geq 4$, the detailed procedure of GM (1, 1) is summarized as follows:

Step 1: The first-order accumulated generating operator is employed to obtain the 1-order accumulation sequence $X^{(1)}$:

$$X^{(1)} = \left\{x^{(1)}(1),\, x^{(1)}(2),\, \ldots,\, x^{(1)}(n)\right\} \tag{1}$$

where

$$x^{(1)}(k) = \sum_{i=1}^{k} x^{(0)}(i),\; k = 1,\, 2,\, \ldots,\, n \tag{2}$$

Step 2: The background value array $Z^{(1)}$ is

$$Z^{(1)} = \left\{z^{(1)}(1),\, z^{(1)}(2),\, \ldots,\, z^{(1)}(n)\right\} \tag{3}$$

where

$$z^{(1)}(k) = 0.5x^{(1)}(k) + 0.5x^{(1)}(k-1),\; k = 2,\, 3,\, \ldots,\, n \tag{4}$$

Step 3: The GM (1, 1) model is

$$x^{(0)}(k) + az^{(1)}(k) = b,\; k = 1,\, 2,\, \ldots,\, n \tag{5}$$

where a is the developing coefficient and b is the grey action.

Step 4: The parameters $\hat{a}$ and $\hat{b}$ can be obtained by the least-square algorithm and written as:

$$\begin{bmatrix} \hat{a} \\ \hat{b} \end{bmatrix} = \left(B^T B\right)^{-1} B^T Y_n \tag{6}$$

$$B = \begin{bmatrix} -z^{(1)}(2) & 1 \\ \vdots & \vdots \\ -z^{(1)}(n) & 1 \end{bmatrix},\; Y_n = \begin{bmatrix} x^{(0)}(2) \\ \vdots \\ x^{(0)}(n) \end{bmatrix} \tag{7}$$

Step 5: The winterization equation of Equation (5) can be written as Equation (8), and its solution, i.e., the time response function, can be written as Equation (9).

$$\frac{dx^{(1)}}{dt} + ax^{(1)} = b \tag{8}$$

$$\hat{x}^{(1)}(k) = \left[x^{(0)}(1) - \frac{\hat{b}}{\hat{a}}\right]e^{-a(k-1)} + \frac{\hat{b}}{\hat{a}} \tag{9}$$

Step 6: The forecasting results can be obtained based on the inverse accumulated generating operator, which can be written as

$$\hat{x}^{(0)}(k) = \begin{cases} x^{(0)}(1),\ k = 1 \\ \hat{x}^{(1)}(k) - \hat{x}^{(1)}(k-1) = (1-e^{\hat{a}})(x^{(0)}(1) - \frac{\hat{b}}{\hat{a}})e^{-a(k-1)},\ k = 2,\ 3,\ \ldots,\ n \end{cases} \tag{10}$$

2.1.2. Artificial Intelligence Optimization Arithmetic

The artificial intelligence optimization arithmetic called manta ray foraging optimization (MRFO), proposed by Zhao et al. [15] in 2020, was developed based on chain foraging, cyclone foraging, and somersault foraging strategies.

Definition 1. *Chain Foraging. Manta rays can identify plankton's position and swim to it. In the foraging process, manta rays form a foraging chain by lining up head-to-tail. All individual manta rays, except the first one, are updated according to the position of food and the ray in front of it, while the first ray is only updated according to the position of the food. The chain foraging can be described as follows:*

$$X_i^d(t+1) = \begin{cases} X_i^d(t) + r\cdot(X_{best}^d(t) - X_i^d(t)) + \alpha\cdot(X_{best}^d(t) - X_i^d(t))\ i = 1 \\ X_i^d(t) + r\cdot(X_{i-1}^d(t) - X_i^d(t)) + \alpha\cdot(X_{best}^d(t) - X_i^d(t))\ i = 2,\ \ldots,\ N \end{cases} \tag{11}$$

$$\alpha = 2\cdot r\cdot\sqrt{|\log(r)|} \tag{12}$$

where $X_i^d(t+1)$ is the ith individual manta ray's position in the dth dimension at time t, $X_{best}^d(t)$ is the position of the best solution thus far in the dth dimension at time t, r is a random vector in [0, 1], and α is a weight coefficient.

Definition 2. *Cyclone Foraging. In the cyclone foraging strategy, the individual manta ray not only swims towards the food along a spiral path, but also follows the one in front of it. The cyclone foraging can be described as follows:*

$$X_i^d(t+1) = \begin{cases} X_{best}^d(t) + r\cdot(X_{best}^d(t) - X_i^d(t)) + \beta\cdot(X_{best}^d(t) - X_i^d(t))\ i = 1 \\ X_{best}^d(t) + r\cdot(X_{i-1}^d(t) - X_i^d(t)) + \beta\cdot(X_{best}^d(t) - X_i^d(t))\ i = 2,\ \ldots,\ N \end{cases} \tag{13}$$

$$\beta = 2e^{r_1\frac{T-t+1}{T}}\cdot\sin(2\pi r_1) \tag{14}$$

where β is a weight coefficient, r_1 is a random vector in [0, 1], and T is the maximum iteration number.

In addition, by randomly defining a new position as the reference position, the individual manta ray is forced to find a new position far from the current best position, which is designed to improve the exploration and enable MRFO to perform an extensive global search. The corresponding mathematical model can be described as follows:

$$X_i^d(t+1) = \begin{cases} X_{rand}^d(t) + r\cdot(X_{rand}^d(t) - X_i^d(t)) + \beta\cdot(X_{rand}^d(t) - X_i^d(t))\ i = 1 \\ X_{rand}^d(t) + r\cdot(X_{i-1}^d(t) - X_i^d(t)) + \beta\cdot(X_{rand}^d(t) - X_i^d(t))\ i = 2,\ \ldots,\ N \end{cases} \tag{15}$$

$$X_{rand}^d = Lb^d + r\cdot(Ub^d - Lb^d) \tag{16}$$

where X_{rand}^d is the reference position randomly defined in the entire search space and Ub^d and *Lb^d are the upper and lower bounds in the dth dimension, respectively.*

Definition 3. *Somersault Foraging. In the somersault foraging strategy, the food's position is considered a pivot. The individual manta ray tends to swim to and from, and around the pivot and somersault to a new position. As a result, they usually update their positions around the best position thus far. The somersault foraging can be described as follows:*

$$X_i^d(t+1) = X_i^d(t) + S\cdot(r_2 \cdot X_{best}^d - r_3 \cdot X_i^d(t)),\ i = 1,\ \ldots,\ N \quad (17)$$

where r_2 and r_3 are random numbers in [0, 1], and S is the somersault factor that is equal to 2, which is defined to decide the manta rays' somersault range.

Pseudocode of the MRFO Algorithm 1.

Algorithm 1 MRFO

Output:
X^*— X with the best fitness
Parameters:
T—the maximum number of iterations
N—the number of population
F_i—the fitness of i-th manta ray
$[L_i, U_i]$ —the boundaries of the i-th variable
X_i—the position of i-th manta ray
t—the current iterations
d—the dimension of the optimized problem.

/*Set the basic parameters of MRFO algorithm. */
/*Initialize the manta ray X_i (i = 1, 2 ... N) randomly. */
FOR EACH i: $1 \le i \le N$ **DO**
  Calculate the fitness F_i for each manta ray
END FOR
/*Determine the best solution found so far X^*. */
WHILE ($t < Iter_{\text{Max}}$) **DO**
  FOR EACH i: $1 \le i \le N$ **DO**
    IF *rand* < 0.5 **DO**
      /* Cyclone foraging strategy. */
      IF $t/T >$ *rand* **DO**
        $X_i^d(t+1) = \begin{cases} X_{best}^d(t) + r\cdot(X_{best}^d(t) - X_i^d(t)) + \beta\cdot(X_{best}^d(t) - X_i^d(t))\ i = 1 \\ X_{best}^d(t) + r\cdot(X_{i-1}^d(t) - X_i^d(t)) + \beta\cdot(X_{best}^d(t) - X_i^d(t))\ i = 2,\ \ldots,\ N \end{cases}$
        $\beta = 2e^{r_1 \frac{T-t+1}{T}} \cdot \sin(2\pi r_1)$
      ELSE IF $t/T \le$ *rand* **DO**
        $X_{rand}^d = Lb^d + r\cdot(Ub^d - Lb^d)$
        $X_i^d(t+1) = \begin{cases} X_{rand}^d(t) + r\cdot(X_{rand}^d(t) - X_i^d(t)) + \beta\cdot(X_{rand}^d(t) - X_i^d(t))\ i = 1 \\ X_{rand}^d(t) + r\cdot(X_{i-1}^d(t) - X_i^d(t)) + \beta\cdot(X_{rand}^d(t) - X_i^d(t))\ i = 2,\ \ldots,\ N \end{cases}$
      END IF
    ELSE IF *rand* > 0.5 **DO**
      /* Chain foraging strategy. */
      $X_i^d(t+1) = \begin{cases} X_i^d(t) + r\cdot(X_{best}^d(t) - X_i^d(t)) + \alpha\cdot(X_{best}^d(t) - X_i^d(t))\ i = 1 \\ X_i^d(t) + r\cdot(X_{i-1}^d(t) - X_i^d(t)) + \alpha\cdot(X_{best}^d(t) - X_i^d(t))\ i = 2,\ \ldots,\ N \end{cases}$
    END IF
  END FOR
  /* Check and modify the new positions based on $[L_i, U_i]$. */
  /* Compute the fitness of each manta ray. */
  IF $F(X_i(t+1)) < F(X_{best})$ **DO**
    /* Update the position of X_{best}, i.e., $X_{best} = X_i(t+1)$. */
  END IF
FOR EACH i: $1 \le i \le N$ **DO**

Algorithm 1 *Cont.*

$X_i^d(t+1) = X_i^d(t) + S\cdot(r_2\cdot X_{best}^d - r_3\cdot X_i^d(t)),\ i = 1,\ \ldots,\ N$
/* Check and modify the new positions based on [$\boldsymbol{L_i}$, $\boldsymbol{U_i}$]. */
/* Compute the fitness of each manta ray. */
IF $F\ (X_i(t+1)) < F\ (X_{best})$ **DO**
/* Update the position of $X_{best,}$ i.e., $X_{best} = X_i(t+1)$. */
END IF
ELSE FOR
$T = t + 1$
END WHILE
RETURN ***the best solution found so far X****

2.1.3. The GM (1, 1) Model Based on the Cycle Prediction Theory: C-GM (1, 1) Model

Although the traditional GM (1, 1) can directly provide multistep forecasting results, it may only perform better in the first step and performs worse as the forecasting horizon increases, which could ultimately lead to a poor forecasting performance. It is worth noting that the most recent data can describe the latest development trend and study the object's characteristics [16]. As a result, this study introduces the cycle prediction theory into the traditional GM (1, 1) model to develop an effective model for multistep forecasting, which can capture the latest development trends and features of the studied object and consequently improve the forecasting performance to a considerable extent. The detailed procedure of the GM (1, 1) model based on cycle prediction theory, denoted as C-GM (1, 1) model, is described as follows:

Step 1: The first-order accumulated generating operator is employed to obtain the 1-order accumulation sequence $X^{(1)}$ as shown in Equation (1);

Step 2: The background value array $Z^{(1)}$ as shown in Equation (3);

Step 3: The parameters $\hat{a}$ and $\hat{b}$ can be obtained by the least-square algorithm, and then the winterization equation and its solution, i.e., the time response function, can be obtained as shown in Equations (8) and (9), respectively;

Step 4: The forecasting model can be obtained based on the inverse accumulated generating operator, which can be written as shown in Equation (10);

Step 5: Cycle prediction theory is introduced to develop an effective model for multi-step forecasting. Specifically, the developed forecasting model is applied to forecast the $n + 1^{\text{th}}$ data point, denoted as y_{n+1}. Then, to utilize the most recent data to predict future data points, the first data point in $X^{(0)}$ is removed, and the forecasting results of the $n + 1^{\text{th}}$ data point, i.e., y_n+_1, are appended into $X^{(0)}$ to reconstruct a new sequence, denoted as X_{n+1}:

$$X_{n+1} = \left\{x^{(0)}(2), x^{(0)}(3), \ldots, x^{(0)}(n),\ y_{n+1}\right\} \tag{18}$$

Accordingly, the reconstructed sequence can be considered as a new nonnegative original time series, and Steps 1 to 5 are repeated to obtain the forecasting results:

$$y_{n+2},\ y_{n+3},\ \ldots,\ y_{n+N},\ N = 1,\ 2,\ 3, \cdots \tag{19}$$

Step 6: Determine if the termination conditions are met. If $n + N \geq m$, the cycle prediction is terminated, and then forecasting results are output y_i, $i = n + 1, n + 2, m$, where m is the length of the forecasted point. Otherwise, Steps 1–5 should be repeated until the termination conditions are reached.

2.1.4. The Newly Developed Forecasting Model: C-MRFO-GM (1, 1) Model

The proposed C-GM (1, 1) model is applicable and effective for multistep forecasting. However, there are two main parameters in the GM (1, 1) model, i.e., a and b, that are usually determined by the least square estimation method that may directly affect the forecasting performance. Most importantly, the solution of the least square estimation method might not be the optimal solution and may result in a poor forecasting performance or inability to obtain the optimal forecasting performance. An artificial intelligence optimization algorithm, inspired by Du et al. [17], Hao et al. [18], Tian and Hao [19] and Yang et al. [20], may be a promising approach for determining the optimal parameters that play a vital role in the development of an optimal model. Accordingly, the MRFO algorithm was employed to determine the optimal parameters in the GM (1, 1) model in the cycle prediction process, i.e., a and b, which can enhance the forecasting model's effectiveness. To obtain improvements in the forecasting performance, the commonly used evaluation metric, mean absolute percentage error (MAPE), was considered the optimization target to improve the forecasting accuracy.

2.2. Part II: The Designed Health Economic Losses Assessment Model

2.2.1. Selection of Pollution Factors, Exposure Populations and Health Effects

Economic losses can be calculated after defining the pollution factors, exposure populations, and health effects. In this paper, the research object, i.e., PM_{10}, is considered as pollution factor. The year-end permanent population were used as the exposed populations to haze pollution. Based on the data availability, the death mortality, respiratory disease outpatient rate, increase of emergency cases, restricted activity days, increase of cases of lower respiratory tract infection/asthma in children, increase of asthma cases and increased cases of chronic bronchitis are considered the health effects in this study.

2.2.2. The Newly Proposed Health Economic Losses Assessment Model

The economic losses caused by air pollution to human health include the following three aspects: losses from premature death due to illness, medical expenses due to illness, and losses due to lost work. The detailed calculation model can be defined as follows:

Definition 4. *Losses from Premature Death Due to Illness*

$$L_1 = N \times P \times n \times a \times S \times G \tag{20}$$

where N is the number of exposure populations, P is the change in premature death caused by increasing one unit of air pollutant concentration, n is the difference between the actual value and reference value of the pollutant concentration, a is the labor force ratio, S is the mean residual life, which is defined as 5 according to Zeng et al. [21], and G *is the per capita annual salary.*

Definition 5. *Medical Expenses Due to Illness*

$$L_2 = \sum X_i \times C_i \tag{21}$$

$$X_i = N \times r_i \times n \tag{22}$$

where X_i is the change value of ith disease due to the variation of pollutant concentration, C_i is the average medical charge of ith disease, and r_i is the morbidity of ith disease caused by increasing one unit of air pollutant concentration.

Definition 6. *Losses Due to Lost Work. The losses due to lost work refers to economic losses caused by certain restrictions on work activities due to air pollution. Based on the research results in Cai [22], one restricted activity day is equivalent to 1/4 days of absence due to illness. The losses due to lost work can be calculated as follows:*

$$L_3 = A \times G_d \tag{23}$$

$$A = \frac{1}{4} \times N \times a \times D \times n \tag{24}$$

where A is the days of lost work due to pollution, $\mathrm{G_d}$ is per capita daily wage, and D is the changes in restricted activity days caused by increasing one unit of air pollutant concentration.

Definition 7. *Total Health Economic Losses. According to the change value of the public health effect due to the variety of pollutant concentrations, the health economic losses caused by air pollutants can be assessed and the detailed model can be defined as follows:*

$$L = \sum_{i=1}^{n} L_i \tag{25}$$

where L is the total health economic losses due to the current condition of air pollutants, L_i is the health economic losses value of the ith public health effect, and n is the number of public health effects.

3. Empirical Study

3.1. Study Area and Data Description

Xi'an, the capital of Shaanxi and the eastern gateway to China's ancient Silk Road, is a national historic and cultural city and is northwest China's largest central city. Its location is shown in Figure 1. Monthly PM_{10} concentration data of Xi'an collected from March 2014 to February 2019 were used in this study, and were retrieved from the website of the China Air Quality Online Monitoring and Analysis platform (https://www.aqistudy.cn accessed on 1 October 2019). In general, the season has a large impact on the concentration of atmospheric pollutants. Therefore, in this paper, one year (i.e., four seasons) was divided according to the general division of the Northern Hemisphere and the actual climate change in China as follows: spring (March–May), summer (June–August), autumn (September–November), and winter (December–February).

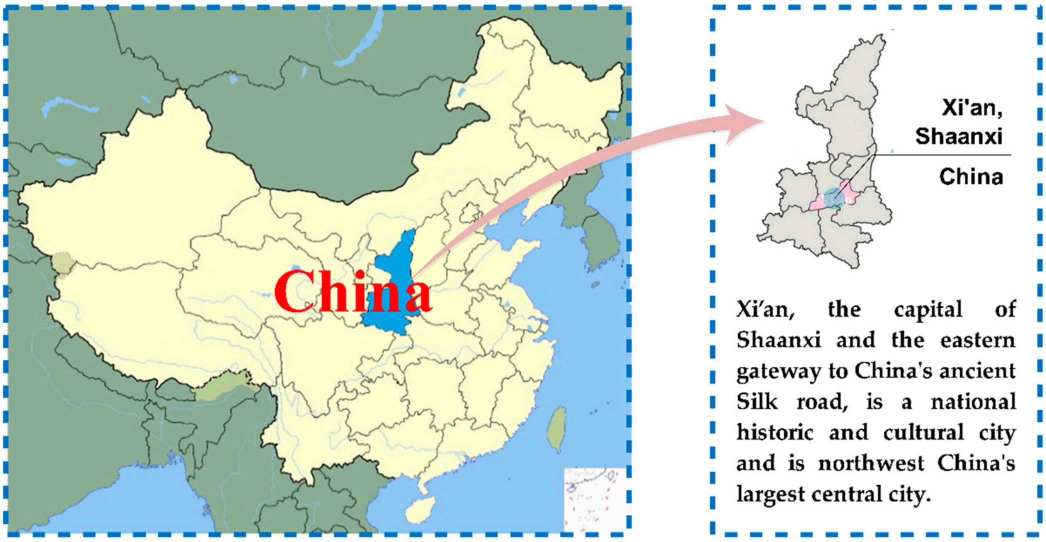

Figure 1. Specific location of the study area.

Based on this, the annual average value of the air pollutant concentration from 2014 to 2018 was calculated and is shown in Table 1. Meanwhile, the limit value of the air pollutant concentration in the national ambient air quality standards (GB 3095-2012) and the exceeding standard rate (ESR) are also presented in Table 1. Level 2 of the pollutant concentration limit was selected for PM_{10} in this study. The annual average concentration of PM_{10} exhibits a roughly decreasing trend year by year with an increase in 2016. The concentration of PM_{10} is the largest in the past five years (2014–2018), which indicates that PM_{10} was not effectively controlled in 2016. Fortunately, the concentration of PM_{10} was effectively controlled after 2016, dropping to 110.67 ug/m^3 and 99.17 ug/m^3 in 2018, respectively. However, the concentration of PM_{10} is still higher than the national standard annual average concentration. Specifically, the ESR value exhibits a roughly decreasing trend year by year but still exceeds the standard limit. As a result, Xi'an needs to continue to strengthen the control of PM_{10} emissions, while the public also needs to strengthen pollution prevention and health protection.

Table 1. Annual average concentration of PM_{10} and exceeding standard rate.

Year	PM_{10}
2014	136.08
ESR	94.40%
2015	129.08
ESR	84.40%
2016	146.17
ESR	108.81%
2017	110.67
ESR	58.10%
2018	99.17
ESR	41.67%
Limit	70

Note: ESR is exceeding the standard rate.

3.2. Results of the Developed C-MRFO-GM (1, 1) Model

3.2.1. Analysis of the Applicability of the GM (1, 1) Model

To develop an effective air pollution forecasting model, the grey prediction theory was used because of its desirable performance with forecasting issues with limited data. To date, the grey model has developed with many variants proposed based on similar modeling procedures of GM (1, 1), such as NDGM (1, 1) [23], NGBM (1, 1) [24], Grey Verhulst [25] and FANGBM [26]. The classical GM (1,1) model and its variants are widely employed in many fields, such as energy consumption [27,28], wind turbine capacity [29], and CO_2 emissions [30]. Since there are so many grey models, the selection of a basic forecasting engine is important for the effectiveness of the developed forecasting model. As a result, in this study, the GM (1, 1), NDGM [23], NGBM (1, 1) [24], Grey Verhulst [25], OP-NGBM (NGBM optimized by MRFO), and OP-FANGBM (FANGBM optimized by MRFO) were considered candidates for basic forecasting engines.

To evaluate the performance of the candidate models, the absolute percentage error (APE) and MAPE were selected, and are defined as follows:

$$\mathrm{APE}(k) = \left| \frac{x^{(0)}(k) - \hat{x}^{(0)}(k)}{x^{(0)}(k)} \right| \times 100\% \tag{26}$$

$$\mathrm{MAPE} = \frac{1}{n} \sum_{k=1}^{n} \left| \frac{x^{(0)}(k) - \hat{x}^{(0)}(k)}{x^{(0)}(k)} \right| \times 100\% \tag{27}$$

where $x^{(0)}(k)$ is the kth data in the original time series, $\hat{x}^{(0)}(k)$ is the corresponding fitted or predicted value and n is the length of the time series. The benchmark of modeling accuracy evaluation by Lewis [31], which has been widely used in different forecasting fields, was employed in this study, and is presented in Table 2.

Table 2. Lewis' benchmark of modeling accuracy evaluation.

MAPE	≤10%	10–20%	20–50%	≥50%
Evaluation	Highly accurate	Good	Reasonable	Inaccurate

Table 3 provides the fitted results and predicted results of GM, NDGM, NGBM, Grey Verhulst, OP-NGBM, and OP-FANGBM for forecasting PM_{10}. The MAPE values of GM, NDGM, NGBM, Grey Verhulst, OP-NGBM, and OP-FANGBM are lower than 10%, which indicates that the modeling accuracy evaluation results of all the models are highly accurate. Table 3 shows that the OP-FANGBM model obtains the best fitting performance for PM_{10}. However, it does not follow that the OP-FANGBM model is more applicable than other grey models for forecasting PM_{10}. In general, the forecasting performance of one model is evaluated based on the forecasting results of the out-sample. However, on the one hand, there are no out-sample data for model forecasting performance evaluation; on the other hand, this study focuses on developing an effective forecasting model for forecasting the future changes in PM_{10} in the next few years. Therefore, in this study, the selection of a basic forecasting engine depends on the rationality of forecasting trends in the next few years, and the MAPE values of the fitted results were introduced as auxiliary means for the models with rational forecasting trends. For example, from the forecasting results of the different models in Table 3, the NGBM, Grey Verhulst, OP-NGBM and OP-FANGBM models present a clear downward trend with a high rate of decline. Combined with the actual situation of air quality, this is inconsistent with the actual trend of change. In addition, the NDGM forecast that the concentration of PM_{10} will remain at 90 ug/m^3 is unrealistic. As a result, the NDGM, NGBM, Grey Verhulst, OP-NGBM and OP-FANGBM models are not applicable for forecasting future changes in PM_{10}. Meanwhile, it can be seen in Table 3 that although it does not achieve the best fitting performance, the GM model not only obtains rational forecasting trends but was also evaluated as highly accurate according to Lewis' benchmark of modeling accuracy evaluation. In addition, comparison of the NGBM model and OP-NGBM model shows that the forecasting result of the OP-NGBM model is more rational than the individual NGBM model. That is, the basic forecasting model can be further improved to develop an effective model that will obtain more rational forecasting results. Finally, we can reasonably conclude that the GM (1, 1) model was more applicable than the other models. As a result, the GM (1, 1) model was selected as the basic forecasting engine and will be combined with other advanced techniques to develop an effective forecasting model for solving forecasting issues in this paper.

Table 3. Results of different models for PM_{10}.

Year	PM_{10}	GM (1, 1)		NDGM (1, 1)		NGBM (1, 1)		Grey Verhulst		OP-NGBM		OP-FANGBM	
		Value	APE	Value	APE	Value	APE	Value	APE	Value	APE	Value	APE
2014	136.08	136.08	0	135.16	0.6761	136.08	0	136.08	0	136.08	0	136.08	0
2015	129.08	139.66	8.1965	140.96	9.2036	129.07	0.0077	112.59	12.775	129.08	0	129.08	0
2016	146.17	126.6	13.3885	125.13	14.3942	137.4	5.9999	141.69	3.0649	134.16	8.2165	133.95	8.3601
2017	110.67	114.75	3.6866	114.26	3.2439	120.77	9.1262	130.09	17.5477	120.46	8.8461	118.81	7.3552
2018	99.17	104.02	4.8906	106.78	7.6737	94.07	5.1427	89.11	10.1442	99.17	0	99.17	0
2019	-	94.29	-	101.65	-	67.88	-	49.5	-	77.3	-	78.92	-
2020	-	85.47	-	98.12	-	46.67	-	24.35	-	58.15	-	59.86	-
2021	-	77.48	-	95.7	-	31.13	-	11.26	-	42.73	-	42.77	-
2022	-	70.23	-	94.04	-	20.36	-	5.06	-	30.9	-	27.96	-
2023	-	63.66	-	92.89	-	13.16	-	2.24	-	22.1	-	15.44	-
2024	-	57.7	-	92.11	-	8.44	-	0.99	-	15.69	-	5.07	-
2025	-	52.31	-	91.57	-	5.38	-	0.43	-	11.08	-	-3.35	-
MAPE			6.0324		7.0383		4.0553		8.7064		3.4125		3.1431

3.2.2. Forecasting Results and Analysis of the Developed Forecasting Model

To provide effective forecasting results of PM_{10} in the future, this study developed a forecasting model based on the GM (1, 1), MRFO algorithm, and cycle prediction strategy. The fitting and forecasting results of GM (1, 1) and the developed model for forecasting PM_{10} are listed in Table 4. Table 4 shows that the developed model obtains the best fitting performance for PM_{10}. Specifically, the MAPE values of GM (1, 1) and the developed model for modeling PM_{10} are 6.0324% and 4.2546%, respectively. As a result, we can reasonably conclude that the developed model performs better than the individual GM (1, 1) model in the fitting performance and forecasting future changes of PM_{10}.

Table 4. Results of GM (1, 1) and the developed model for PM_{10}.

Year	PM_{10}	GM		Developed Model	
		Value	APE	Value	APE
2014	136.08	136.08	0	136.08	0
2015	129.08	139.66	8.1965	129.09	0.0077
2016	146.17	126.6	13.3885	118.23	19.1147
2017	110.67	114.75	3.6866	108.29	2.1505
2018	99.17	104.02	4.8906	99.17	0
2019		94.29	-	90.83	-
2020		85.47	-	82.27	-
2021		77.48	-	74.53	-
2022		70.23	-	67.95	-
2023		63.66	-	61.68	-
2024		57.7	-	56.04	-
2025		52.31	-	50.95	-
MAPE			6.0324		4.2546

From Table 4, it is observed that the average annual concentrations of PM_{10} from 2019 to 2025 are 90.83, 82.27, 74.53, 67.95, 61.68, 56.04, and 50.95, respectively. In addition, the changing trend of PM_{10} from 2014 to 2025 is shown in Figure 2. It shows a slightly decreasing trend from 2019 to 2025. According to the abovementioned analysis, the concentration of PM_{10} is beyond the limit values from 2019 to 2021, which indicates that the influence of PM_{10} on public health may end in 2022. As a result, Xi'an city should adopt more effective and persistent air quality control measures to control the emissions of PM_{10} and try their best to end the influence before 2022.

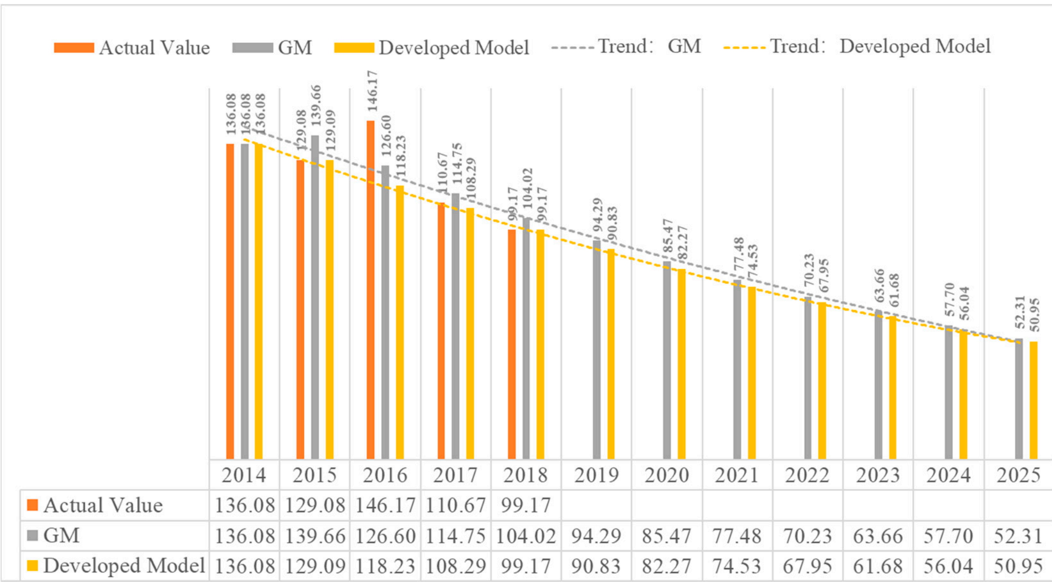

Figure 2. The changing trend of PM_{10} from 2014 to 2025.

3.2.3. Remark for the Performance of Different Models

The applicability of the GM (1, 1) model is discussed and approved by comparing the forecasting results of GM (1, 1) model with NDGM, NGBM, Grey Verhulst, OP-NGBM, and OP-FANGBM model. It should be noted that, under the optimistic situation of air pollution control, the annual average concentration of PM_{10} will decrease year by year, and the rate of decrease will become slower and slower. In other words, the annual average concentration level of PM_{10} is unlikely to drop rapidly, and it is also unlikely that it will remain almost unchanged for many years. Therefore, at the stage of selecting the basic forecasting model, the first consideration should be given to whether the model captures the possible and reasonable future change trend of PM_{10}. Based on analysis in Section 3.2.1, only the GM (1, 1) model provides the reasonable trend in the future, which is selected as the basic model of the developed model. On the premise that the GM (1, 1) model can provide a reasonable trend, the research goal of this paper has changed from the rationality of forecasting trend to the superiority of forecasting performance. As a result, the C-MRFO-GM (1, 1) model is developed to forecast the annual average concentration of PM_{10} from 2019 to 2025. Then the fitting and forecasting results of GM (1, 1) and the developed model are compared in Section 3.2.2. By comparing the GM (1, 1) model and the developed model, it can be observed that the developed model achieves the best results in terms of MAPE. Based on abovementioned analysis, we can safely draw the conclusion that the developed model can achieve effective forecasting of PM_{10} from 2019 to 2025, which not only performs better than GM (1, 1) model in terms of forecasting results' accuracy but also exhibits significant superiority compared with NDGM, NGBM, Grey Verhulst, OP-NGBM, and OP-FANGBM model in terms of the forecasting trend's rationality.

3.3. Results of the Designed Health Economic Losses Evaluation Model

In this section, the evaluation of the health effects of PM_{10} and the corresponding economic losses are divided into two parts as follows: evaluation for the past and evaluation for the future. This can help the public understand the basic conditions of the health effects and economic losses, and provide the conditions for the public to avoid damages to health and economic losses in the future. Most importantly, politicians can adjust their policies according to the results of the evaluation for the future.

3.3.1. Data Sources for Health Economic Losses Assessment

For the empirical study for Xi'an, China, the data source for the proposed health economic losses assessment model are as follows: (1) concentration: actual value for 2014 to 2018, and forecasting results of the developed model in Section 3.2.2; (2) the threshold value of PM_{10}: see Section 3.3.2; (3) exposure population: represented by the year-end permanent population, collected from Statistical Bulletin National Economic and Social Development of Xi'an 2014–2018; (4) labor force ratio: equals social workers divided by the year-end permanent population, in which the number of social workers can be collected from Xi'an Statistical Yearbook 2018 and women and children planning monitoring report of Xi'an 2018; (5) per capita annual salary: represented by average wages of urban non-private employees by industry, collected from Xi'an Statistical Yearbook 2018 and the related statistical data released by Xi'an Bureau of Statistics; (6) per capita daily wage: equals per capita annual salary divided by the days of one year; (7) per capita medical expenses: the values in 2013 can be found in Zeng et al. [21], and then the values in other years can be adjusted and obtained according to consumer price index, in which the consumer price index can be collected from the Statistical Bulletin National Economic and Social Development of Xi'an 2014–2018.

3.3.2. Selection of Threshold Value of PM_{10}'s Health Effects

To evaluate the health effect of air pollution and the corresponding economic losses, the concentration threshold value of PM_{10} should be determined. However, there is no standard for the threshold of air pollutant concentration in the research. In some studies, such as Li et al. [32], the standard is selected from the World Health Organization [33]. According to the related studies conducted by Li et al. [34–36], four baseline values of the annual concentration of PM_{10} are considered as the background value and shown in Table 5. Interim target-1 (IT-1) equals the limit value of air pollutant concentration in the national ambient air quality standards (GB 3095-2012). Therefore, in the current situation in which interim target-1 (IT-1) is still not achieved, 70 ug/m^3 is selected as the threshold value of PM_{10}.

Table 5. Four annual mean concentration baseline levels of PM_{10}.

Level	PM_{10} (ug/m^3)
Interim target-1 (IT-1)	70
Interim target-2 (IT-2)	50
Interim target-3 (IT-3)	30
Air quality guidelines (AQG)	20

Note: The World Health Organization suggested progressive achievement of four pollution thresholds which cascade down through three interim targets (IT-1: 70 μg/m^3; IT-2: 50 μg/m^3; IT-3: 30 μg/m^3) to reach the ultimate target, i.e., 20 μg/m^3 [37].

3.3.3. Evaluation of the Past: 2014 to 2018

The public health effects caused by air pollution and the corresponding economic losses from 2014 to 2018 were estimated based on the dose-response functions between the changes in PM_{10} concentration and the health effects shown in Table 6 [21], and the final evaluation results are presented in Table 7. According to the evaluated results shown in Table 7, the detailed analysis is as follows:

Table 6. Dose-response functions between the changes in PM_{10} concentration and the health effects.

Heath Effect Ends	Changed Values (One in 1,000,000 People)
Death mortality	6
Respiratory disease outpatient rate	12
Increase of emergency cases	235
Restricted activity days	57,500
Increase of cases of lower respiratory tract infection/asthma in children	23
Increase of asthma cases	2068
Increased cases of chronic bronchitis	61

(1) The change values of the public health effects in 2014 (2018) show that the number of premature deaths was the smallest with the value of 3421 (1751), while the number of days of lost work was the largest with the value of 5,062,207 (2,604,808); from the corresponding economic losses in 2014 (2018), the health economic losses caused by medical expenses was the smallest with the value of 3.6096 hundred million Yuan (1.9512 hundred million Yuan) and the health economic losses caused by delayed wages was the largest with the value of 7.5688 hundred million Yuan (5.9819 hundred million Yuan). The total health economic losses in 2014 (2018) were 16.9444 hundred million Yuan (12.4900 hundred million Yuan).

(2) Under the baseline levels of PM_{10}, the change values of the public health effects in 2018 were lower than those in the other four years. Furthermore, the total health economic losses caused by PM_{10} from 2014 to 2018 were 16.9444, 16.3875, 23.4475, 15.2293, and 12.4900 hundred million Yuan, respectively. More specifically, the health economic losses in the past five years were 84.4987 hundred million Yuan. More details about the influence of PM_{10} on public health can be seen in Table 7.

Table 7. Results of the public health effects caused by PM_{10} and the corresponding economic losses from 2014 to 2018.

Year.	Concentration (ug/m^3)	Basic Materials and Data				Per Capita Medical Expenses (Yuan)			Public Health Effects Caused by Air Pollution					Health Economic Losses (Hundred Million Yuan)			
									Change Values of Each Heath Effect								
		Exposure Population (Ten Thousand)	Labor Force Ratio (%)	Per Capita Annual Salary (Yuan)	Per Capita Daily Wage (Yuan)	Asthma	Respiratory Tract Infection	Increased Cases of Chronic Bronchitis	Premature Death	Asthma	Respiratory Tract Infection	Increased Cases of Chronic Bronchitis	Days of Lost Work	Premature Death	Medical Expenses	Delayed Wages	Total Losses
2014	136.08	862.75	61.77	54,573	149.52	202.80	608.40	811.20	3421	1,178,978	153,928	34,776	5,062,207	5.7660	3.6096	7.5688	16.9444
2015	129.08	870.56	60.66	60,557	165.91	204.22	612.66	816.88	3086	1,063,628	138,868	31,374	4,484,682	5.6678	3.2792	7.4405	16.3875
2016	146.17	883.21	61.05	67,205	183.62	206.06	618.17	824.23	4036	1,391,229	181,640	41,037	5,903,718	8.2793	4.3278	10.8404	23.4475
2017	110.67	961.67	62.00	75,262	206.20	210.18	630.54	840.71	2347	808,818	105,600	23,858	3,485,630	5.4756	2.5664	7.1873	15.2293
2018	99.17	1000.37	62.10	83,821	229.65	214.17	642.52	856.69	1751	603,459	78,788	17,800	2,604,808	4.5570	1.9512	5.9819	12.4900
Total									14,641	5,046,112	658,824	148,845	21,541,045	29.7457	15.7341	39.0188	84.4987

3.3.4. Evaluation of the Future: 2019 to 2021

The public health effects caused by air pollution and the corresponding economic losses from 2019 to 2021 were estimated and are presented in Table 8. In Table 8, Total I is the total public health effects and corresponding health economic losses from 2016 to 2020, which can be used to present the health damage from air pollution and the health economic losses conditions from 2016 to 2020. In addition, relevant decision makers can make policy adjustments according to the planning targets and the predicted values for the next two years to ensure the successful completion of the 13th Five-Year Plan (i.e., the plan, objectives, and their implementation for national economic and social development over five years from 2016 to 2020, here is the environmental protection related goals). Total II is the total public health effects and corresponding health economic losses from 2021 to 2025, which can be used to present the health damage from air pollution and the health economic losses conditions in China's 14th Five Year Plan (i.e., the plan, objectives, and their implementation for national economic and social development over five years from 2021 to 2025). Similarly, relevant decision makers can formulate a reasonable 14th Five Year Plan according to the forecasting results of public health effects and corresponding health economic losses from 2021 to 2025 to ensure the continuous improvement of air quality in the period of the 14th Five Year Plan. Total III is the total public health effects and corresponding health economic losses from 2019 to 2025, which can be used to present the health damage from air pollution and the health economic losses condition in the next few years.

The change values of the public health effects in 2019 show that the number of premature deaths was the smallest (1331), while the number of days of lost work was the largest (1,997,420); from the corresponding economic losses in 2019, it can be observed that the health economic losses caused by medical expenses was the smallest (1.5121 hundred million Yuan) and the health economic losses caused by delayed wages was the largest (5.1228 hundred million Yuan). The total health economic losses in 2019 were 10.5373 hundred million Yuan. Similar findings and analyses can be performed and determined for other years. The detailed evaluation results of each year can be seen in Table 8. Under the baseline levels of PM_{10}, the change values of the public health effects and corresponding health economic losses in 2021 were lower than those in other years. Specifically, the results showed that the total health economic losses caused by PM_{10} from 2019 to 2021 are 10.5373, 7.3338, and 3.2058 hundred million Yuan, respectively. In addition, it is worth noting that it is expected that there may be no health damages or health economic losses from PM_{10} after 2021. In other words, the influence of PM_{10} on public health may end in 2022.

Table 8. Results of the public health effects caused by air pollution and the corresponding economic losses from 2019 to 2021.

Year.	Concentration (ug/m^3)	Basic Materials and Data				Per Capita Medical Expenses (Yuan)			Public Health Effects Caused by Air Pollution					Health Economic Losses (Hundred Million Yuan)			
									Change Values of Each Heath Effect								
		Exposure Population (Ten Thousand)	Labor Force Ratio (%)	Per Capita Annual Salary (Yuan)	Per Capita Daily Wage (Yuan)	Asthma	Respiratory Tract Infection	Increased Cases of Chronic Bronchitis	Premature Death	Asthma	Respiratory Tract Infection	Increased Cases of Chronic Bronchitis	Days of Lost Work	Premature Death	Medical Expenses	Delayed Wages	Total Losses
2019	90.83	1064.93	62.64	93,611.70	256.47	218.35	655.05	873.39	1331	458,735	59,893	13,531	1,997,420	3.9024	1.5121	5.1228	10.5373
2020	82.27	1133.66	63.19	104,545.99	285.64	222.61	667.82	890.43	835	287,660	37,557	8485	1,263,472	2.7580	0.9667	3.6090	7.3338
Total I									10,300	3,549,901	463,478	104,711	15,255,048	24.9723	11.3242	32.7414	69.0379
2021	74.53	1206.83	63.74	116,757.47	319.01	226.95	680.84	907.79	328	113,056	14,761	3335	500,911	1.2205	0.3874	1.5980	3.2058
Total II									328	113,056	14,761	3335	500,911	1.2205	0.3874	1.5980	3.2058
Total III									2494	859,451	112,211	25,351	3,761,803	7.8809	2.8662	10.3298	21.0769

4. Discussion of the Influence of the Threshold Value of PM_{10}

Under the baseline of the national standard limited concentration values, the influence of PM_{10} on public health may end in 2022. However, if we select the baseline levels of PM_{10} with lower concentrations, the average annual concentration of PM_{10} will still impact human health and cause health economic losses. For example, by selecting four annual mean concentrations of PM_{10} shown in Table 5 as the baseline, the total health economic losses caused by PM_{10} from 2016 to 2020 is 69.0379 hundred million Yuan under IT-1, 113.3141 hundred million Yuan under IT-2, 157.5929 hundred million Yuan under IT-3 and 179.7343 hundred million Yuan under AQG, the total health economic losses caused by PM_{10} from 2021 to 2025 is 3.2058 hundred million Yuan under IT-1, 52.5630 hundred million Yuan under IT-2, 155.2636 hundred million Yuan under IT-3 and 206.6086 hundred million Yuan under AQG, and the total health economic losses caused by PM_{10} from 2019 to 2025 is 21.0769 hundred million Yuan under IT-1, 92.5021 hundred million Yuan under IT-2, 217.2708 hundred million Yuan under IT-3. The forecasting results of PM_{10} show that under the baseline of IT-2, the influence of PM_{10} on public health may end in 2026, while under the baseline of IT-3 and AQG, PM_{10} will still pose a negative impact on public health and cause economic losses from 2019 to 2025.

5. Conclusions

This study began by posing the following question: When will the influence of PM_{10} on public health end? To answer this question, by combining the newly proposed forecasting model and evaluation model, a novel hybrid framework is developed for forecasting, evaluation and early-warning for the influence of PM_{10} on public health. These are the main contributions of this study. To verify the effectiveness of the developed hybrid framework to address air pollution issues and answer the research question, the PM_{10} concentration data in Xi'an, China was employed in the case study. Furthermore, the results demonstrated that the developed hybrid framework is applicable in China and may become a promising technique that enriches the current research and meets the requirements of air quality management and haze governance. It should be noted that this study mainly focused on answering the question in China. As a result, the "replicability" of our work in the international context is not considered in this study. However, the empirical results prove the validity of the established research framework in forecasting, evaluation, and early-warning for the influence of PM_{10} on public health. Therefore, we can safely draw the conclusion that the developed framework can be considered as an effective tool in the international context. Furthermore, considering the availability of data and the significance of internationalization, the international context research can be the subject of our future studies, which will be a worthwhile studying direction for the whole society.

Specifically, the new findings from this study that are different from the literature can be summarized as follows:

(1) Based on the results of the empirical study, the question "When will the influence of PM10 on public health end?" can be answered as follows: The influence of PM_{10} on public health may end in 2022 under the baseline of the national standard limited concentration values, but it will still pose a negative impact on public health and cause economic losses from 2019 to 2025 under the baseline of IT-2, IT-3 and AQG. Overall, the current situation is not very good, and Xi'an city should adopt more effective and persistent air quality control measures to control PM_{10} emissions.

(2) Different from most previous air pollution health economic losses studies that focused on $PM_{2.5}$, the present study focused on PM_{10}, which has been neglected in previous studies and can bridge the research gap in air pollution health economic losses. The experimental results show that the changes in health effects and health economic losses caused by PM_{10} cannot be ignored, and people should consider emissions reduction and control of PM_{10}.

(3) This study contributes forecasting, evaluation and early-warning to the research, which are new ideas and a new research framework. Specifically, forecasting can provide future changes in PM_{10}, while evaluation can help the public understand the basic conditions of health effects and economic losses and also predict the future conditions for the public. Most importantly, politicians can adjust their policies according to the results of the evaluation for the future. To the best of our knowledge, most previous economic losses assessment studies only focused on assessing the economic costs of past disasters while ignoring the significance of evaluating the economic losses for the past and future. As a result, the presented research framework and ideas provide a theoretical reference and academic reference for future research. In the future, the research framework and ideas based on forecasting, evaluation and early-warning can be extended and applied in other fields, such as storm surge disaster losses [38], e-commerce precision poverty alleviation benefit assessment [39], rainstorm disaster losses [40], earthquakes and flood losses [41] and impacts of haze pollution on the tourism industry [42].

(4) Most previous studies focused on health economic losses caused by air pollution in different areas and at different times. On the positive side, assessing past economic losses provides support for air pollution prevention and control. However, when will the influence of air pollution on public health end? This is a significant and neglected issue, which can be considered a new research direction. As a result, this study takes PM_{10} as the research object and first poses the question: "When will the influence of PM_{10} on public health end?" The answer is provided based on forecasting, evaluation and early-warning.

(5) Another interesting finding is that the traditional grey model is more applicable than other grey models for forecasting PM_{10} in Xi'an, China. In general, in the air quality forecasting field and other related forecasting fields, variants of the traditional grey model may perform better than the traditional grey model. For example, in Wu et al. [43], the GM (1, 1) model with fractional order accumulation performs better than the GM (1, 1) model alone. Different from previous studies, this study not only considers the fitting accuracy but also the rationality of the future development trend of things. It should be noted that the prediction of the future development trend needs to conform to the development law of things, which is obviously different from the training and testing process of the prediction model.

(6) Wu and Zhao (2019) [44] employed an individual model named the fractional order accumulation GM (1, 1) model to forecast the number of lightly polluted days from 2017–2020, which proves the forecasting power of grey forecasting theory. Cycle prediction theory can capture the latest development trend and features of the studied object, while optimization can obtain the model's optimal parameters. As a result, cycle prediction theory and optimization can improve the forecasting performance to a large extent. Considering the advantages and disadvantages of grey forecasting theory, this study further develops the findings of Wu and Zhao (2019) and introduces cycle prediction theory and optimization into air pollution's health economic losses assessment and forecasting.

Author Contributions: Conceptualization, W.Y. and J.W.; Formal analysis, W.Y.; Funding acquisition, J.W.; Investigation, G.T.; Methodology, W.Y. and G.T.; Software, W.Y.; Supervision, J.W.; Validation, Y.H.; Visualization, G.T.; Writing — original draft, W.Y. and Y.H.; Writing — review & editing, Y.H. All authors have read and agreed to the published version of the manuscript.

Funding: This research was funded by National Office for Philosophy and Social Sciences: the Major Program of National Social Science Foundation of China (grant number 17ZDA093).

Institutional Review Board Statement: Not applicable.

Informed Consent Statement: Not applicable.

Data Availability Statement: Publicly available datasets were analyzed in this study. Detailed data sources can be found in Sections 3.1 and 3.3.1.

Acknowledgments: The authors are grateful to the anonymous reviewers and the editor for their constructive comments and suggestions for this paper.

Conflicts of Interest: The authors declare no conflict of interest.

References

1. García Nieto, P.J.; Sánchez Lasheras, F.; García-Gonzalo, E.; de Cos Juez, F.J. PM10 concentration forecasting in the metropolitan area of Oviedo (Northern Spain) using models based on SVM, MLP, VARMA and ARIMA: A case study. *Sci. Total Environ.* **2018**, *621*, 753–761. [CrossRef]
2. Turner, M.C.; Krewski, D.; Pope, C.A.; Chen, Y.; Gapstur, S.M.; Thun, M.J. Long-term ambient fine particulate matter air pollution and lung cancer in a large cohort of never-smokers. *Am. J. Respir. Crit. Care Med.* **2011**, *184*, 1374–1381. [CrossRef]
3. Ostro, B.D.; Eskeland, G.S.; Sanchez, J.M.; Feyzioglu, T. Air pollution and health effects: A study of medical visits among children in Santiago, Chile. *Environ. Health Perspect.* **1999**, *107*, 69–73. [CrossRef] [PubMed]
4. Saini, J.; Dutta, M.; Marques, G. Fuzzy Inference System Tree with Particle Swarm Optimization and Genetic Algorithm: A novel approach for PM10 forecasting. *Expert Syst. Appl.* **2021**, *183*, 115376. [CrossRef]
5. Xu, Y.; Yang, W.; Wang, J. Air quality early-warning system for cities in China. *Atmos. Environ.* **2017**, *148*, 239–257. [CrossRef]
6. Li, R.; Jin, Y. The early-warning system based on hybrid optimization algorithm and fuzzy synthetic evaluation model. *Inf. Sci.* **2018**, *435*, 296–319. [CrossRef]
7. Zhu, S.; Qiu, X.; Yin, Y.; Fang, M.; Liu, X.; Zhao, X.; Shi, Y. Two-step-hybrid model based on data preprocessing and intelligent optimization algorithms (CS and GWO) for NO_2 and SO_2 forecasting. *Atmos. Pollut. Res.* **2019**, *10*, 1326–1335. [CrossRef]
8. Liu, H.; Xu, Y.; Chen, C. Improved pollution forecasting hybrid algorithms based on the ensemble method. *Appl. Math. Model.* **2019**, *73*, 473–486. [CrossRef]
9. Hao, Y.; Tian, C. The study and application of a novel hybrid system for air quality early-warning. *Appl. Soft Comput. J.* **2019**, *74*, 729–746. [CrossRef]
10. Xu, X. Forecasting air pollution $PM_{2.5}$ in Beijing using weather data and multiple kernel learning. *J. Forecast.* **2020**, *39*, 117–125. [CrossRef]
11. Fan, G.F.; Guo, Y.H.; Zheng, J.M.; Hong, W.C. A generalized regression model based on hybrid empirical mode decomposition and support vector regression with back-propagation neural network for mid-short-term load forecasting. *J. Forecast.* **2020**, *39*, 737–756. [CrossRef]
12. Fang, Y.; Guan, B.; Wu, S.; Heravi, S. Optimal forecast combination based on ensemble empirical mode decomposition for agricultural commodity futures prices. *J. Forecast.* **2020**, *39*, 877–886. [CrossRef]
13. Wang, J.; Du, P.; Lu, H.; Yang, W.; Niu, T. An improved grey model optimized by multi-objective ant lion optimization algorithm for annual electricity consumption forecasting. *Appl. Soft Comput. J.* **2018**, *72*, 321–337. [CrossRef]
14. Lu, K.H.; Hong, C.M.; Han, Z.; Yu, L. New intelligent control strategy hybrid grey-RCMAC algorithm for ocean wave power generation systems. *Energies* **2020**, *13*, 241. [CrossRef]
15. Zhao, W.; Zhang, Z.; Wang, L. Manta ray foraging optimization: An effective bio-inspired optimizer for engineering applications. *Eng. Appl. Artif. Intell.* **2020**, *87*, 103300. [CrossRef]
16. Zhao, H.; Guo, S. An optimized grey model for annual power load forecasting. *Energy* **2016**, *107*, 272–286. [CrossRef]
17. Du, P.; Wang, J.; Yang, W.; Niu, T. A novel hybrid model for short-term wind power forecasting. *Appl. Soft Comput. J.* **2019**, *80*, 93–106. [CrossRef]
18. Hao, Y.; Tian, C.; Wu, C. Modelling of carbon price in two real carbon trading markets. *J. Clean. Prod.* **2020**. [CrossRef]
19. Tian, C.; Hao, Y. Point and interval forecasting for carbon price based on an improved analysis-forecast system. *Appl. Math. Model.* **2020**, *79*, 126–144. [CrossRef]
20. Yang, W.; Wang, J.; Niu, T.; Du, P. A hybrid forecasting system based on a dual decomposition strategy and multi-objective optimization for electricity price forecasting. *Appl. Energy* **2019**, *235*, 1205–1225. [CrossRef]
21. Zeng, X.; Wang, T.; Li, Y. Economic loss of air pollution in Xi'an City. *J. Arid Land Resour. Environ.* **2015**, *29*, 105–110. [CrossRef]
22. Cai, H.D. *Modern Environmental Hygiene*; People's Medical Publishing House: Beijing, China, 1995.
23. Xie, N.M.; Liu, S.F.; Yang, Y.J.; Yuan, C.Q. On novel grey forecasting model based on non-homogeneous index sequence. *Appl. Math. Model.* **2013**, *37*, 5059–5068. [CrossRef]
24. Pao, H.T.; Fu, H.C.; Tseng, C.L. Forecasting of CO_2 emissions, energy consumption and economic growth in China using an improved grey model. *Energy* **2012**, *40*, 400–409. [CrossRef]
25. Liu, S.; Dang, Y.; Fang, Z.; Xie, N. *Grey System Theory and Its Application*; Science Press: Beijing, China, 2010.
26. Wu, L.; Zhao, H. Using FGM(1,1) model to predict the number of the lightly polluted day in Jing-Jin-Ji region of China. *Atmos. Pollut. Res.* **2019**, *10*, 552–555. [CrossRef]
27. Ma, X.; Mei, X.; Wu, W.; Wu, X.; Zeng, B. A novel fractional time delayed grey model with Grey Wolf Optimizer and its applications in forecasting the natural gas and coal consumption in Chongqing China. *Energy* **2019**, *178*, 487–507. [CrossRef]
28. Ma, X.; Liu, Z. The GMC(1, n) model with optimized parameters and its application. *J. Grey Syst.* **2017**, *29*, 122–138.

29. Xia, J.; Ma, X.; Wu, W.; Huang, B.; Li, W. Application of a new information priority accumulated grey model with time power to predict short-term wind turbine capacity. *J. Clean. Prod.* **2020**, *244*, 118573. [CrossRef]
30. Wang, Z.X.; Li, Q. Modelling the nonlinear relationship between CO_2 emissions and economic growth using a PSO algorithm-based grey Verhulst model. *J. Clean. Prod.* **2019**, *207*, 214–224. [CrossRef]
31. Lewis, C.D. *Industrial and Business Forecasting Method*; Butter-worth-Heinemann: London, UK, 1982.
32. Li, L.; Lei, Y.; Wu, S.; Huang, Z.; Luo, J.; Wang, Y.; Chen, J.; Yan, D. Evaluation of future energy consumption on $PM_{2.5}$ emissions and public health economic loss in Beijing. *J. Clean. Prod.* **2018**, *187*, 1115–1128. [CrossRef]
33. World Health Organization. WHO Air Quality Guidelines for Particulate Matter, Ozone, Nitrogen Dioxide and Sulfur Dioxide. Global Update 2005. Summary of Risk Assessment 2006. Available online: https://apps.who.int/iris/handle/10665/69477 (accessed on 6 August 2021).
34. Li, L.; Lei, Y.; Wu, S.; Chen, J.; Yan, D. The health economic loss of fine particulate matter ($PM_{2.5}$) in Beijing. *J. Clean. Prod.* **2017**, *161*, 1153–1161. [CrossRef]
35. Li, H.; Liu, Z.; Liu, K.; Zhang, Z. Predictive Power of Machine Learning for Optimizing Solar Water Heater Performance: The Potential Application of High-Throughput Screening. *Int. J. Photoenergy* **2017**, 4194251. [CrossRef]
36. Li, J.S.; Chen, G.Q.; Chen, B.; Yang, Q.; Wei, W.D.; Wang, P.; Dong, K.Q.; Chen, H.P. The impact of trade on fuel-related mercury emissions in Beijing—evidence from three-scale input-output analysis. *Renew. Sustain. Energy Rev.* **2017**, *75*, 742–752. [CrossRef]
37. Ielpo, P.; Paolillo, V.; de Gennaro, G.; Dambruoso, P.R. PM_{10} and gaseous pollutants trends from air quality monitoring networks in Bari province: Principal component analysis and absolute principal component scores on a two years and half data set. *Chem. Cent. J.* **2014**, *8*, 14. [CrossRef] [PubMed]
38. Liu, Q.; Ruan, C.; Zhong, S.; Li, J.; Yin, Z.; Lian, X. Risk assessment of storm surge disaster based on numerical models and remote sensing. *Int. J. Appl. Earth Obs. Geoinf.* **2018**, *68*, 20–30. [CrossRef]
39. Guan, H.; Zhao, A.; Shi, G. *Research on E-Commerce Precision Poverty Alleviation*; Economic Science Press: Beijing, China, 2019.
40. Tan, L.; Wu, X.; Xu, Z.; Li, L. Comprehensive economic loss assessment of disaster based on CGE model and IO model—A case study on Beijing "7.21 Rainstorm.". *Int. J. Disaster Risk Reduct.* **2019**, *39*, 101246. [CrossRef]
41. Dabbeek, J.; Silva, V.; Galasso, C.; Smith, A. Probabilistic earthquake and flood loss assessment in the Middle East. *Int. J. Disaster Risk Reduct.* **2020**, *49*, 101662. [CrossRef]
42. Hao, Y.; Niu, X.; Wang, J. Impacts of haze pollution on China's tourism industry: A system of economic loss analysis. *J. Environ. Manage.* **2021**, *295*, 113051. [CrossRef]
43. Wu, L.; Li, N.; Yang, Y. Prediction of air quality indicators for the Beijing-Tianjin-Hebei region. *J. Clean. Prod.* **2018**, *196*, 682–687. [CrossRef]
44. Wu, W.; Ma, X.; Zeng, B.; Wang, Y.; Cai, W. Forecasting short-term renewable energy consumption of China using a novel fractional nonlinear grey Bernoulli model. *Renew. Energy* **2019**, *140*, 70–87. [CrossRef]